Power Conservation and Quality of Surveillance in Target Tracking Sensor Networks *

Chao Gui and Prasant Mohapatra
Computer Science Department
University of California, Davis
Davis, CA 95616
{guic,prasant}@cs.ucdavis.edu

ABSTRACT

Target tracking is an important application of wireless sensor networks. In this application, the sensor nodes collectively monitor and track the movement of an event or target object. The network operations have two states: the surveillance state during the absence of any event of interest, and the tracking state which is in response to any moving targets. Thus, the power saving operations, which is of critical importance for extending network lifetime, should be operative in two different modes as well. In this paper, we study the power saving operations in both states of network operations. During surveillance state, a set of novel metrics for quality of surveillance is proposed specifically for detecting moving objects. In the tracking state, we propose a collaborative messaging scheme that wakes up and shuts down the sensor nodes with spatial and temporal preciseness. This study, which is a combination of theoretical analysis and simulated evaluations, quantifies the trade-off between power conservation and quality of surveillance while presenting guidelines for efficient deployment of sensor nodes for target tracking application.

Keywords: Sleep Planning, Quality of Surveillance, Coverage Process, Proactive Wakeup,

1. INTRODUCTION

A wireless sensor network (WSN) can be formed when a set of micro-sensors with embedded processing unit and radio transceiver are deployed in a given space. Since the first-hand sensor readings can be collected and processed within the network, WSN can revolutionize the manner how people can monitor the environment. In the near future, we can expect deployment of sensor networks for a wide range of applications, such as environmental monitoring, battle field surveillance, machinery diagnosis and planetary exploration.

*This research was supported in part by the National Science Foundation under the grants CCR-0296070 and ANI-0296034.

Due to the wide range of application areas, sensor networks present a variety of network operation models for data delivery and processing. Three models are identified in [21], namely, the *continuous, event-driven and user-initiated*. In this paper, we focus on the second type, which represents applications like surveillance and target tracking. In this type of application, the user is only interested in the occurrence of a certain event or a set of events. The possible examples of interesting events could be movement of an intruder, movement of wild life in forest or reservoirs, or movement of enemy tanks in battle fields.

In most cases, power sources in the sensor nodes are non-refreshable. Thus, power saving operations at each node play a critical role in extending the network life-time. In target tracking applications, the "interesting" events happen infrequently with long intervals of inactivity. The monitoring sensor network should remain at a certain level of vigilance, as well as work in unattended manner for as long as possible. The sensor nodes can stay in sleeping mode during the long intervals of inactivity. Thus, the network operations have two states. One is the surveillance state during which there are no events of interest in the field, but the sensors are ready to detect any possible occurrences. The other state is the tracking state during which the network reacts in response to any moving targets, and the sensors are collaborating in measuring the target's path and speed.

Power conservation and the quality of surveillance are two conflicting requirements of target tracking sensor networks. With unlimited power supply, a given area can be monitored perfectly with a set of sensor nodes that cover the entire area in terms of sensing. However, since the sensor nodes have limited power, the quality of monitoring becomes inversely proportional to the life time of the network.

In this paper, we attempt to formalize and analyze the trade-off between power conservation and quality of surveillance in target tracking sensor networks. In the process, we also develop and evaluate new sleep-awake planning scheme for target tracking sensor networks. For the surveillance state, we develop a sleep plan for each sensor node as a schedule for when to turn into the sleep mode. In the context of network life-time, the more each node stays in the sleep mode, the less energy is consumed per unit time for the network. On the other hand, from a spatial perspective, sleep plan directly governs the distribution as well as the number of the

active sensors in the field at any given time. Lower nodal alertness will reduce the network's quality of monitoring. In order to analyze the trade-off between the two issues quantitatively as well as qualitatively, we first propose a metric for the level of surveillance within the network. It quantifies the network's quality of surveillance in a partially covered network field. Current research efforts on coverage [3, 12, 26] have focused on full coverage of the target field. However, in many cases, the deployment cost, the physical limitations, and the operational efficiency justify a partial coverage of the target field. For a target tracking sensor network, though intensive coverage is needed at the time and location of the target event, partial coverage is enough during the surveillance state.

The spatial effect of sleep planing leads to the notion of "soft deployment" of sensor nodes. We assume the following two-step sensor deployment model. First, the sensors are physically deployed with redundant density and in an ad hoc manner. Then, the sleep plan turns off the spare sensors into sleep mode to prolong the network's life-time. Thus, the remaining active sensors at any given time present a certain spatial distribution pattern. This approach is called the "soft deployment" of sensors, which can be flexibly tuned and changed after the sensors are physically deployed. One goal of this paper is to propose a framework for different types of soft deployment methods, and study their performance in terms of energy savings and quality of surveillance.

In target tracking application, a proactive wake-up protocol is also needed in addition to the power conservation protocol. The goal is to assure that all the nodes within the local area surrounding the target can participate in the tracking, as if the involved nodes are not using power-saving operations.

In summary, the contributions of this paper include the quantification of the trade-off between power conservation and quality of surveillance, the development of efficient sleep-awake protocols, and the evaluation of soft deployment techniques. The formalization and the trade-off analysis provide guidelines for efficient deployment of sensor nodes. The proposed sleep-awake protocol provides better quality of surveillance while reducing the power consumption.

The rest of the paper is organized as follows. In Section 2, we categorize the related research works in current literature. In Section 3, we study the coverage process of the sensing areas of the sensors and present a quality of surveillance metric for partially covered sensor fields. In Section 4, we present a framework of various types of sleep planning methods. A proactive wakeup protocol is presented in Section 5. The detailed results of performance evaluation study are presented in Section 6. Finally, the conclusions and future directions are presented in Section 7.

2. RELATED WORK

Mobile target tracking using large scale sensor networks has been recently under extensive study [1, 7, 13, 25, 29, 31, 32, 33]. Among these research work, [7, 33] present a leader-based tracking scheme using capable sensor nodes, while [1, 13] are two tracking schemes based on the minimalist binary sensor model. In [25, 29], the network architecture is cluster-based so that a cluster-head calculates target location based on signal readings from its slave nodes. Finally, [31] and [32] present a tree-based approach to facilitate sensor collaboration in tracking. In this paper, we refrain from proposing neither a tracking method nor collaboration protocol. Instead, we propose and study power conservation protocols and sensor deployment schemes that are independent of the tracking methods and collaboration protocols.

Besides the tracking protocols, the trade-offs between power conservation and the tracking error are studied in [17]. The results confirm the intuition that significant energy-saving can be obtained while keeping the tracking error within acceptable limits.

2.1 Network Coverage and Surveillance

Sensor network coverage affects the quality of monitoring in the operational field. Different coverage models and solutions are surveyed by Cardei and Wu [3]. To determine the minimum set of sensors for covering every location in the target field, the centralized solutions are based on approximation techniques [2, 20] or on integer programing [5]. In [12], Huang and Tseng provide a solution on how each node using localized information can test the network p-coverage condition, which is true if every point of operational field is covered by at least p sensors. Finally, Wang *et al.* in [26] studied the fundamental relationship of sensing coverage and communication connectivity, assuming different relationships between each nodes sensing range and communication range. As shown in later sections, a partially covered sensor field will do a good job in detecting the occurrence of a moving object, while achieving significantly higher energy savings compared to a fully covered field. Target tracking application is an example to justify the need for studying partially covered field, and defining metric for quantifying the quality of surveillance in such field.

Given the deployment of a set of sensors, the quality of surveillance can also be characterized by an extreme case analysis, which determines the minimal and maximal exposure path within the covered field. The minimal exposure path can be used to identify the least monitored or the maximum breach area of the field. These paths are first identified as quality of service metrics for sensor networks in [15]. Algorithms for finding these extreme paths are under study. The centralized algorithms are presented in [15], while the localized algorithms are presented in [14, 24]. Maximum breach path reveals the weakest monitored region of the field and provides optimum navigation for the target. However, it cannot provide guidelines on the density and distribution of sensors for detecting targets.

2.2 Power Conservation Protocols

Power conservation protocols such as SPAN[6], and ASCENT[4] have been proposed for ad hoc multihop wireless networks. In [16], topology control methods are studied for a two-tiered sensor network architecture. The goal of these works is to reduce the unnecessary energy consumption during the packet delivery process. These protocols are topology oriented and do not consider the geometrical relations and effects.

In [28], the proposed sleep planning protocol let each node decide its own sleep schedule so that certain degree of cov-

erage can be achieved. Moreover, the protocol can achieve differentiated surveillance for certain critical areas within the network field. However, the work does not provide a metric on the quality of surveillance, especially for the partially covered field.

GAF[27] and PEAS[30] are two sleep planning protocols that can be used for soft deployment of sensors. In GAF, sensors use location information to divide the field into fixed square grids. Nodes within a grid switch between sleep and awake, with the guarantee that one node in each grid stays up. The size of the grid can be used to control the density of distribution of active nodes. In PEAS, each node periodically transmits probe messages, and replies to any received probe messages from the neighbor nodes. A node can be off-duty if it receives replies for its probes. In this scheme, the density of the active nodes can be controlled by the range of probing messages. In [18], Schurgers *et al.* studied the trade-off between power conservation and network performance in terms of packet delivery delay. An energy management protocol, STEM, is proposed to work in combination with GAF or SPAN protocols.

In this paper, we include GAF and PEAS into the framework of soft deployment methods, and propose new deployment methods as well. We also use analysis and simulation to study what quality of surveillance can be achieved under different methods.

3. QUALITY OF SURVEILLANCE

The coverage-based metrics measure the level of network surveillance by the statistics of the number of sensor nodes covering each location in the field, where p-coverage means each location is covered by at least p sensors. This is a static metric, not accounting for the possible moving status of an event. The value p is often considered as an integer equal to or greater than 1, which warrants the impossibility of void areas. However, in our target application area, the target that are monitored and therefore being tracked are often moving within the network field. This supports the effort of deriving a surveillance metric that take the moving targets into consideration. Meanwhile, the movement of the targets makes it unnecessary to cover every position of the field, since a network with small and scattered void areas will be able to detect a moving object within a short delay. The advantage is that we can put more nodes into the sleep mode, compared to the full coverage case, and therefore achieve significant savings of energy.

Throughout this paper, we have considered a 2-dimensional planar field for monitoring. However, the proposed approach with substantial enhancements can be adopted for 3-dimensional fields.

3.1 Theoretical Background

We model the deployment of sensor nodes in a given field as a realization of a spatial point process. Formally speaking, a spatial 2-dimensional point process is a stochastic model governing the location of events $\{s_1, s_2, \cdots, s_n\}$ in a bounded area, X, which is a subset of $\mathcal{R}^2$. Let ξ_i denote the location of s_i within X. This is equivalent to deploying node N_i at the position ξ_i within the field. When n is large and the events are distributed independently and uniformly within X, the point process is termed as *homogeneous Poisson process*. A property of this process is that the number of events in any subset S of X is Poisson distributed with mean $\frac{n\|S\|}{\|X\|}$. Here, $\| S \|$ and $\| X \|$ mean the area of S and X, respectively.

We express

$$\mathcal{T}(r) \equiv \{x \in \mathcal{R}^2 : |x| \leq r\} \tag{1}$$

for the closed disc of radius r, centered at the origin, and

$$\xi + \mathcal{T}(r) \equiv \{\xi + x : x \in \mathcal{T}(r)\} \tag{2}$$

for the closed disc centered at ξ. At any given time, sensor node N_i located at ξ_i has a sensing range of r_i, represented by the disc $\xi_i + \mathcal{T}(r_i)$. Thus, the sensing coverage of the network field can be be defined as a sequence of random discs, denoted as $\mathcal{C}$, where

$$\mathcal{C} \equiv \{\xi_i + \mathcal{T}(r_i), 1 \leq i \leq n\}. \tag{3}$$

$\mathcal{C}$ is termed as a *coverage process* by the set of n discs. A point $z \in \mathcal{R}^2$ is said to be covered by the coverage process if it is contained in at least one of the discs $\xi_i + \mathcal{T}(r_i)$.

THEOREM 1. *Consider a coverage process $\mathcal{C}$, and assume that the driving point process is homogeneous with density λ. Let $\mathcal{I}$ be a straight line segment in $\mathcal{R}^2$ of length l. Let α denote the total number of intersections of $\mathcal{I}$ with parts of boundaries of covering discs. Then, the expected number of intersections, denoted by α^*, can be obtained from the following:*

$$\alpha^* = 2\pi^{-1} \cdot \lambda \cdot l \cdot E(|\partial\mathcal{T}(r_i)|), \tag{4}$$

where $\partial\mathcal{T}(r_i)$ denotes the boundary of disc $\mathcal{T}(r_i)$, and $E(|\partial\mathcal{T}(r_i)|)$ denotes the expected length of the disc boundaries.

Theorem 1 is a direct corollary of Theorem 4.3 in [11]. In this theorem, intersections of parts of disc boundaries with $\mathcal{I}$ are counted once for each intersection. Each disc boundary can have one or two intersections with $\mathcal{I}$.

We assume the sensing ranges of the n nodes, $\{r_1, r_2, \cdots, r_n\}$, are *n independently and identically distributed (iid)* random variables, taking values within the range $[r_{min}, r_{max}]$ with mean $\bar{r}$. Then, $E(|\partial\mathcal{T}(r_i)|)$ is equal to $2\pi\bar{r}$. Thus, the mean value of the number of intersections is

$$\alpha^* = 4\lambda \cdot l \cdot \bar{r}. \tag{5}$$

Due to the homogeneity of the driving point process, this result is irrelevant to the position and the orientation of the line segment $\mathcal{I}$, as long as it is well contained within the area X. Note that the Poisson-ness of the driving point process is not used in the proof of this theorem; only homogeneity is required. This means even when $\{\xi_i\}$ are uniformly but not independently distributed within X, this result is still applicable.

3.2 Quality of Surveillance (QoSv) Metric

We first study the basic case in which all nodes remain awake all the time without sleeping. The goal is to estimate the

minimum number of sensor nodes needed to achieve a desirable level of surveillance. By reducing the number of redundant nodes, the cost for sensor network deployment is reduced. Moreover, the results will be applied to the more general case in which the nodes are over-deployed, and we need to decide the minimum number of nodes needed to stay awake in order to achieve a given level of surveillance.

For sensor networks with target tracking application, the first observation is that we do not need to cover every point in the field to achieve a quick detection of moving objects. Because of the continuous change of its location, a moving object, not covered by any sensor in this time stamp, is likely to enter the covered area in the next time stamp. According to the formal definition of target tracking problem given in [19], we assume a target arrives at random time at a random location within the field, and it then moves for random length of time before disappearing. What is the distance traveled by an object remaining uncovered before it intersects with the sensing boundary of a sensor node? This is of central interest to a network engaged in target surveillance, thus we can define the network's $QoSv$ as the following.

Definition 1. ***QoSv(X).*** *Let X be the monitored field, covered by a set of sensor nodes. Let t be a target, which appears at a uniformly random location in the field, moving with continuous free path. Let $\mathcal{L}$ be the traveled distance of t before it is first detected by any sensor, and let $\mathcal{L}^*$ be its expected value. We define quality of surveillance of network on X, denoted as $QoSv(X)$, the reciprocal value of $\mathcal{L}^*$, i.e.,*

$$QoSv(X) \equiv \frac{1}{\mathcal{L}^*}. \tag{6}$$

We are also interested in the amount of time traveled by the intruding object before it gets detected. This value is determined by the $QoSv(X)$ and the target's moving speed.

Given a field X and its sensor network deployment, $QoSv(X)$ is an ideal metric for the network's quality of surveillance. However, it can hardly provide practical use since its value can be very hard to obtain. We are interested in how to quickly estimate the $QoSv(X)$ value. We assume that a target moves with continuous motion and can only move for a short distance before being detected. Thus, a line segment can approximate the target's path before detection. In cases where the target is a vehicle, the approximation will be more accurate. Thus, we can have the following definitions.

Definition 2. ***Linear Uncovered Length.*** *Given the field X, let coverage process $\mathcal{C}$ direct the deployment of the sensor nodes. Let x be a location within X and not covered by any sensor. Let $\mathcal{L}(x,\theta)$ be a line segment starting at position x, with orientation angle θ. The other end point of $\mathcal{L}$ is at the first intersection of $\mathcal{L}$ with any boundary of the covering discs. Thus, the length of $\mathcal{L}(x,\theta)$ defines the Linear Uncovered Length(LUL) at location x with orientation θ.*

Definition 3. ***Average Linear Uncovered Length at location x.*** *This is the length of $\mathcal{L}(x,\theta)$ averaged over all orientation angles. It is denoted as $ALUL(x)$, and*

$$ALUL(x) \equiv \begin{cases} 0 & : \ x \text{ is covered} \\ \frac{\int_0^{2\pi} \mathcal{L}(x,\theta)d\theta}{2\pi} & : \ otherwise \end{cases} \tag{7}$$

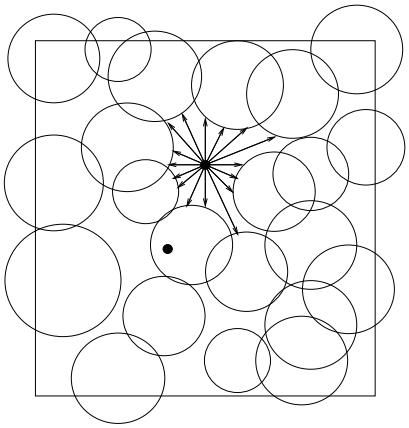

Figure 1: Average Linear Uncovered Length(ALUL) at covered and uncovered points.

Figure 1 illustrates the calculation of ALUL value at two positions in a partially covered field. For the two black dots in the figure, one is on a covered location, thus its ALUL value is zero. The other dot is not covered and its ALUL calculation is illustrated in the figure.

Definition 4. ***Average Linear Uncovered Length of area X.*** *This is the value of $ALUL(x)$ averaged over all locations within the field, and is expressed as*

$$ALUL(X) \equiv \frac{\int_{x \in X} ALUL(x)dx}{\| X \|}, \tag{8}$$

where $\| X \|$ denotes the area of X.

As the result of previous analysis, we propose to use $ALUL(X)$ as the estimation of $\mathcal{L}^*$ in Definition 1. We use the traveled distance instead of the time delay for QoSv metric. The reason is that time delay will also be dependent on the target's moving speed, while traveled distance is independent of the target's speed.

Next, we investigate on the following problem. Given the target field X, and value l as the desired quality of surveillance, what is the minimum number of sensor nodes needed so that if the nodes are independently and uniformly positioned in X, $ALUL(X)$ will be less than or equal to l.

It is inherently a complex problem to calculate $ALUL(X)$. However, Theorem 1 presented in section 3.1 has provided us a theoretical hint on its approximation value. Figure 2 illustrates the geometrical foundation of the following approximation result.

Proposition 1. *Let field X be covered by a homogeneous coverage process $\mathcal{C}$ of random discs, and $\mathcal{I}$ be a line*

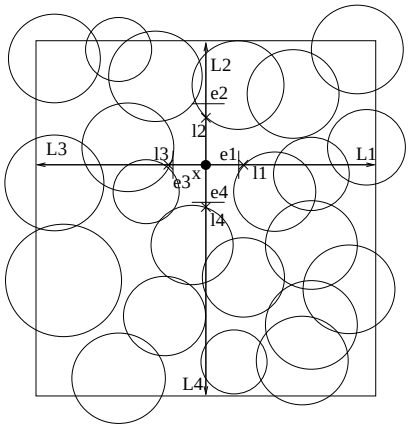

Figure 2: Comparison of LUL value and intersection counts at location x and four directions (east, west, south, north). In this example, L1 is the line segment from x to "east" boundary of field X, and it has 5 intersections with disc boundaries. Value e1 is the length of L1 divided by 5. Also, l1 is the length of line segment from x at the same direction to the first intersection of disc boundaries. The same notations are applied for the other three directions.

segment in X with length l. Let α^* be the expected number of intersections of $\mathcal{I}$ with the boundaries of the covering discs. For any line segment $\mathcal{I}$, the following holds:

$$ALUL(X) \approx \frac{l}{\alpha^*}. \quad (9)$$

We can further propose the following approximating metric.

DEFINITION 5. ***Expected Singular Intersection Length.*** *Given the field X and n sensor nodes, let the deployment of the nodes and their coverage over field X be defined by the coverage process $\mathcal{C}$. Let $\mathcal{I}^*$ be any line segment in X, and the length of $\mathcal{I}^*$ be such that the expected number of intersections of $\mathcal{I}^*$ with the boundaries of covering discs is 1. The length of $\mathcal{I}^*$, $|\mathcal{I}^*|$, defines the Expected Singular Intersection Length of area X, denoted as $ESIL(X)$.*

Combining Theorem 1 and Proposition 1, we can have the following result:

$$QoSv(X) = \frac{1}{ALUL(X)} \approx \frac{1}{ESIL(X)} = \frac{4 \cdot n \cdot \bar{r}}{\| X \|}. \quad (10)$$

3.3 Experimental Results

To study the relationship between the ALUL and the ESIL, defined in Section 3.2, we conduct the following experiment for an operational field to be monitored of size $400m \times 400m$. The sensors are independently and uniformly distributed in the field. To change the node density, we vary the number of sensors from 50 up to 300. We experimented for both the case of equal sensing range, R, and for the case of random sensing range. In the later case, each node chooses a fixed sensing range which is uniformly distributed within the range $[(1-\delta)R, (1+\delta)R]$. For each set of the parameters, a simulation run is repeated 100 times with different random number seeds and different node deployments.

Figure 3(a) shows the results of the equal sensing range case, while Figure 3(b) shows the results of the random sensing range case. The sensing range R is 20 meters and δ is chosen as 0.1. The y-axis in both figures is the reciprocal value and the reciprocal relation shows a linear point pattern. The solid lines in both figures show the reciprocal value of ESIL, which is proportional to the number of deployed nodes. Starting from 50 deployed nodes, the calculated ALUL values are very close to the ESIL values. This is true in both equal sensing range case and the random sensing range case. This result verifies that ESIL can be a close estimate of ALUL. As the number of nodes increases beyond a threshold value, this close match no longer hold. As shown in the two figures, the threshold for equal sensing range case is 180 nodes, and that of the random case is 120 nodes. At the threshold density, the ESIL values for both cases are 11.11 meters and 16.67 meters, respectively, which are comparable to the sensing range of 20 meters. Beyond this threshold, the ALUL values are significantly smaller than the ESIL values.

We now look at the reason behind this result. The calculated ALUL value is the value of $ALUL(x)$ averaged over all locations in the field. For any covered location x, $ALUL(x)$ equals zero. Thus, in a mostly covered field with small patches of uncovered locations, the ALUL value of the field is of small value. In both figures, we also show the values of $ALUL(x)$ averaged only over uncovered locations. This is denoted as ALUL' value in the both figures. In both cases, ALUL' values do not deviate far from the ESIL values, regardless of node density. We also observe a sudden drop in ALUL values in the figures, which is the result of phase transition phenomenon in this coverage process. Theoretical studies on unit disc coverage process [9, 10] prove the existence of a critical density, beyond which all the clumps of covered areas are connected into one clump and occupies the most of the space.

Finally, we can have the following inference from the experiment study. When the ALUL is higher than a certain reasonable length, and the resulting node density is less than a threshold, the ESIL value can be very close to ALUL. Thus, ESIL serves as a good approximation for $QoSv$. At the threshold, the quality of surveillance metric value is smaller but close to the sensing range, and the required node density gives a less than but close to full coverage of the field. With higher requirements beyond threshold, ESIL becomes a conservative metric.

4. SLEEP PLANNING AND SOFT DEPLOYMENT OF SENSOR NODES

For a target tracking sensor network, the sensor coverage requirements at the surveillance state and at the tracking state differ significantly. The surveillance state requires a homogeneous coverage on a wide area, but does not need full coverage. The tracking state requires an intense coverage (covered by at least p sensors simultaneously), but only covers a certain small area at each time stamp.

To satisfy both the requirements while minimizing energy

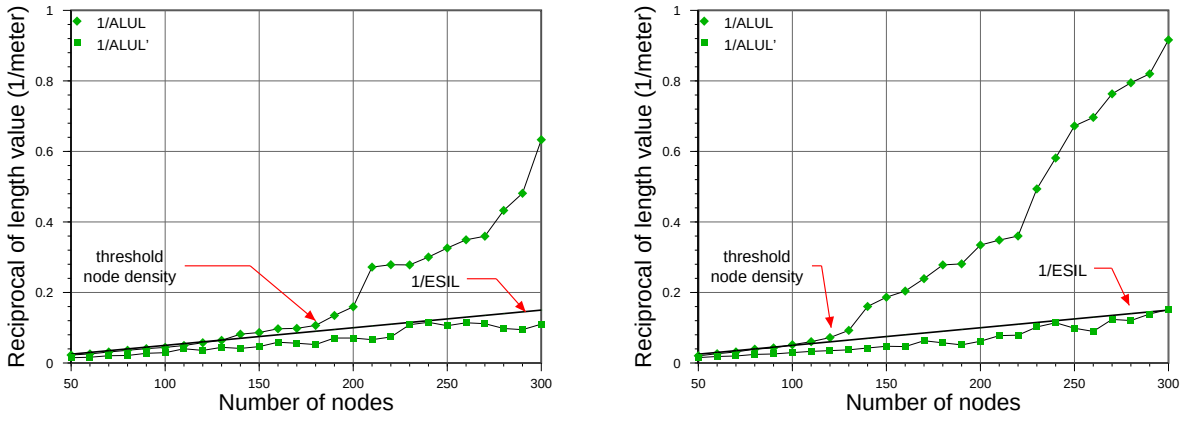

(a) Equal sensing range.

(b) Random sensing range ($\delta = 0.1$).

Figure 3: Comparison of ALUL and ESIL.

consumption, we can use a two-step sensor deployment method. Sensors are physically deployed according to the tracking state coverage requirement. Normally, each point within the field should be covered by at least p sensors, termed as p-coverage provisioning. Most of the time, the network works in surveillance state in an unattended manner. Only a subset of nodes needs to be turned on at any given time, thus the active node density can be specified by the quality of surveillance metrics proposed in the Section 3.2. This control of the density and distribution of active nodes by sleep planning protocols is termed as "sensor soft deployment". The physical deployment cannot be easily changed once the network is deployed. However, by tunning the sleep planning protocol, the soft deployment can be flexibly changed upon new requirements.

In this section, we study the different methods of using sleep planning to achieve the goals of sensor soft deployment. From the intended sensor distribution patterns, we can form the following two categories: the *uniform distribution methods* and the *planned distribution methods*. The only requirement for Equation-10 in Section 3.2 to hold true is that the active nodes be distributed uniformly within the field X. Physically, the sensor deployment may not be uniform due to various real-life limitations. Within reasonable range, this distribution distortion can be amended by sleep planning that achieves a uniform distribution of active nodes. Methodologies in this category induces *pre-scheduled independent sleeping*, and *neighbor collaboration sleeping*. The scheme proposed in [28] belongs to the first method, while GAF [27] and PEAS [30] belong to the second method. Another category of sleep planning can achieve a certain sensor distribution pattern at planned locations. With location information, only nodes at planned locations remain active. With the planned distribution, we can have a more deterministic guarantee of the $QoSv$ metrics.

4.1 Uniform Distribution Methods

4.1.1 *Pre-scheduled Independent Sleeping*

This scheme allows each of the deployed nodes set up its own sleep schedule during network initialization. During the operation time, each node independently follows its own sleep schedule, without collaborating with each other on the sleeping issues. The most basic pre-scheduled independent sleeping can be implemented by a Random Independent Sleeping (RIS) scheme. At each node, the time is divided into time slots of equal length, T_{slot}. The interval of each time slot is divided into two parts: the active period and the sleeping period. The duration of active period is $p \cdot T_{slot}$, and the sleeping period takes the remaining part of a time slot. Randomness must be introduced to the boundaries of time slots of all the sensor nodes. That is, the start point of the time slots at all the nodes should be randomly and independently distributed. The inherent asynchronization of the clocks at the nodes will help in implementing this randomness. However, in order to "magnify" the clock asynchronization to the time scale of T_{slot}, each node should initially choose a random delay before starting the very first time slot. For each node, the initial delay is a random variable uniformly distributed in $[0, T_{slot}]$. By random independent sleeping, each node has a probability of p for being active at any given time. In a macroscopic view, the expected number of active nodes within the area X at any given time is $p \cdot N$, and the subset of active nodes are distributed uniformly within X. Once the active node number, n^*, is decided, the active probability of each node, p, can be derived by the following equation.

$$p = \frac{n^*}{N}. \tag{11}$$

Besides alertness, T_{slot} is another parameter of the RIS scheme. We will study the impact of T_{slot} on QoSv in Section 6.

4.1.2 *Neighborhood Cooperative Sleeping (NCS)*

To achieve the goal of deciding which subset of sensors should be awake and working, one can use a Neighborhood Co-

operative Sleeping (NCS) scheme. An NCS scheme called PEAS was proposed in [30]. Initially, each node sleeps for an exponentially distributed duration. The probability density function is $f(t_s) = \lambda e^{-\lambda t_s}$, where λ is the probing rate and t_s denotes the sleeping time duration. When a node wakes up, it begins probing the environment by broadcasting a PROBE message. The transmission power of the message is controlled so that the message reaches the desired transmission range[1]. Any working node upon receiving the PROBE message should respond with a REPLY message. The probing node then waits for a duration indicated by a parameter *Probe_ Wait_ Time* to collect REPLY messages. This is the Probing Environment(PE) scheme. If no working nodes are found, the probing node starts working. Otherwise, it returns to the sleep mode for another amount of time. The length of the next sleeping time is decided by the Adaptive Sleeping(AS) algorithm, using the local information collected during the probing process. By changing the probing range, PEAS can control the density of the working nodes.

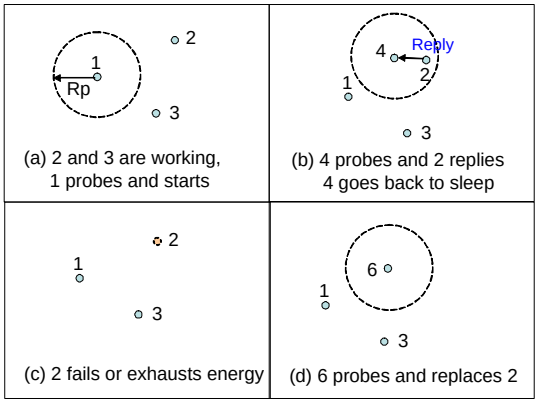

Figure 4: Example of operations in PECAS protocol.

In PEAS, a working node remains awake continuously until its physical failure or depletion of battery power. The other sleeping nodes then replace any failed nodes as needed. This working model may not be desirable, because the density of functional sensor nodes will drop down as time progresses. Furthermore, the failure of nodes (due to energy depletion) may cause partitioning of the network or isolation of nodes. In an environment where the major cause of sensor failure is the depletion of energy, it is desirable to balance energy consumption among the neighboring nodes. To achieve this goal, a node should change to the sleep mode after working for a given time and the neighboring nodes take turns to serve in the working mode.

We propose an extension to the PEAS scheme, named as Probing Environment and Collaborating Adaptive Sleeping(PECAS). Using the example shown in Figure 4, we illustrate the operations of PECAS protocol. The PE scheme is the same as that of the PEAS scheme. As shown in Figure 4(a), when node 1 wakes up and probes, no other nodes are active within its probing range, thus node 1 will remain active. We now describe our extension. Every node remains within the working mode only for a duration indicated by parameter *Work_ Time_ Dur*. Each node has a variable *Next_ Sleep_ Time*. When a node starts working, it sets the *Next_ Sleep_ Time* as the current time plus *Work_ Time_ Dur*, so that *Next_ Sleep_ Time* indicates the time-stamp this working node will stop working and go to sleep. When a working node responds to a PROBE message, the value of *Next_ Sleep_ Time* timer is attached to the REPLY message. For the example shown in Figure 4(b), node 2 is active and it hears the probing packet sent out by node 4. As node 2 replies to node 4, it will include its *Next_ Sleep_ Time* timer value. The probing node, which has collected one or more REPLY messages, then chooses the length of its next sleep duration. Since the node keeps a record of the earliest *Next_ Sleep_ Time* value among the collected REPLY messages, the next sleep duration is the earliest *Next_ Sleep_ Time* value minus the current time. Using method, we assure that when a working node begins sleeping, other sleeping node(s) in the neighborhood will wakeup and probe. An example is shown in Figures 4(c) and (d), in which node 2 goes to sleep and a nearby node (node 6) wakes up and takes its role. It is possible that several neighbor nodes around a working node know its next sleep time, and they may all wake up at the same time and contend with the probing packets. To prevent this situation, a random offset value ϵ can be added to the probing node's next wake time. For the example shown in Figure 4, when node 4 knows node 2's *Next_ Sleep_ Time*, it will wake up at time $Next\_Sleep\_Time + \epsilon_4$. Also, node 6 behaves similarly, and set next wake up time as $Next\_Sleep\_Time + \epsilon_6$. In this example, node 6 chooses a smaller offset value than node 4, and succeeds in the contention.

[1] Typical sensor motes, such as MICA2 MOTE by Crossbow company, support variable transmission power.

4.2 Planned Distribution Methods

By the uniform distribution soft-deployment, the ALUL metric for quality of surveillance can only be satisfied statistically, i.e., satisfaction with probabilistic guarantee. Using a planned distribution soft-deployment method, the ALUL metric can be satisfied with deterministic guarantee. We assume each sensor node knows its location accurately. Only nodes at planned locations remain active so that the distribution of all active nodes forms a planned pattern. In this section, we use a 2-D mesh as the distribution pattern, which is shown in Figure 5. The horizontal and vertical solid lines in the figure shows a virtual 2-D mesh on the monitored field. Distance between each adjacent horizontal (vertical) lines is l_G. For i-th horizontal line, sensors with x-coordinates within the range $[i \cdot l_G - \delta, i \cdot l_G + \delta]$ will remain active. Same is true for the j-th vertical line. With the sensing range of each sensor being r, each line forms a stripe of a covered area of width $2r + 2\delta$. Each uncovered area in this sensor deployment is a square, the side of which is of length l_U. Thus, we have

$$l_U = l_G - 2r - 2\delta \tag{12}$$

Given the values for l_G, r and δ, we now derive the ALUL value of area X covered in this 2-D mesh sensor deployment.

THEOREM 2. *Let $\mathcal{S}$ be an uncovered area with convex boundary. We use $\partial\mathcal{S}$ to denote the boundary of $\mathcal{S}$, and $|\partial\mathcal{S}|$ to denote the length of the boundary. Let x be any point*

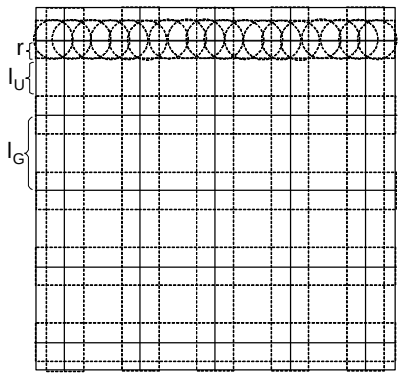

Figure 5: 2D mesh pattern of planned sensor distribution.

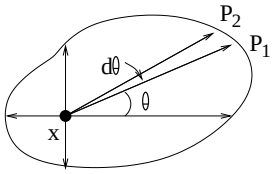

Figure 6: The ALUL value at any point within a convex shape.

within $\mathcal{S}$, and we have

$$ALUL(x) = \frac{|\partial \mathcal{S}|}{2\pi} \tag{13}$$

Proof Since x is in uncovered area, by definition, we have

$$ALUL(x) = \frac{\int_0^{2\pi} \mathcal{L}(x,\theta)d\theta}{2\pi}, \tag{14}$$

where $\mathcal{L}(x,\theta)$ is the linear uncovered length at x on direction θ. From Figure 6, we have $\mathcal{L}(x,\theta) \cdot d\theta$ equals to the length of arc $\widetilde{P_1P_2}$ on $\partial\mathcal{S}$. Thus, we have

$$\int_0^{2\pi} \mathcal{L}(x,\theta)d\theta = |\partial \mathcal{S}| \tag{15}$$

Thus the result of this theorem will hold.

Theorem 3. *Let X be the monitored field of size $L \times L$. The physical deployment of sensors is modeled by a homogeneous coverage process of adequate density. The covering discs are of uniform radius, r. The distribution of active sensors follows the 2-D mesh planned pattern shown in Figure 5. Then, we have*

$$ALUL(X) = \frac{2}{\pi}(\lfloor \frac{L}{l_G} \rfloor)^2 \frac{(l_G - 2r - 2\delta)^3}{L^2} \tag{16}$$

Proof With adequate sensor density, each uncovered region within field X becomes a square of size $l_U \times l_U$. For any position x within an uncovered region, applying Theorem 2, we have

$$ALUL(x) = \frac{4 \cdot l_U}{2\pi} \tag{17}$$

By definition of $ALUL(X)$, we have

$$ALUL(X) = \frac{2 \cdot l_U}{\pi} \times \frac{\parallel Uncovered\ regions \parallel}{\parallel X \parallel} \tag{18}$$

Studying Figure 5, we have

$$\parallel Uncovered\ regions \parallel = m \cdot l_U^2, \tag{19}$$

where

$$m = (\lfloor \frac{L}{l_G} \rfloor)^2 \tag{20}$$

Integrating all above equations, we can derive the main result of this theorem.

If the sensors on the horizontal and vertical lines are working continuously, and the other sensors never need to wakeup, the active nodes will finally deplete their energy, and the mesh structure will no longer exist. Thus, we need to evenly spread the energy consumption around all nodes. Instead of one static mesh, we can form multiple meshes all covering the whole field, and switch among the meshes at intervals. Thus, the time is divided into slots of length T_{slot}. Each setup of the 2-D mesh will serve for one time slot. At the end of a slot, each horizontal mesh line will offset by value of 2δ downward. The bottom-most horizontal line may need to wrap to the top of the field. Similar is applied to the vertical mesh lines. With this swapping scheme among several 2-D mesh setups, the energy consumption of all nodes are fairly spread-out. One caveat of this swapping is that it requires time synchronization among the sensor nodes. This requirement for the target tracking sensor network can be achieved by approaches proposed in [8, 23].

5. PROACTIVE WAKEUP FOR TRACKING

Consider a distributed sensor network monitoring a large operational area. The network operations have two stages: the surveillance stage during the absence of any event of interest, and the tracking stage which is in response of any moving targets. From a sensor node's point of view, it should initially work in the low-power mode when there is no targets in its proximity. However, it should exit the low-power mode and be active continuously for certain amount of time when a target enters its sensing range, or more optimally, when a target is about to enter within a short period of time. Finally, when the target passes by and moves further away, the node should decide to switch back to the low-power mode. In Section 4, we have discussed the sleep planning of each node during the surveillance stage. In this section, we deal with how each node wakes up and sleeps during the tracking stage.

Intuitively, a sensor node should enter the tracking mode and remain active when it senses a target during a wake-up period. However, it is possible that a node's sensing range is passed by a target during its sleep period, so that the target can pass across a sensor node without being detected by the node. Thus, it is necessary that each node be proactively informed when a target is moving towards it.

In this section, we develop the Proactive Wakeup (PW) algorithm. Each sensor node has four working modes: Waiting, Prepare, SubTrack, and Tracking mode. The Waiting mode represents the low power mode in surveillance stage. Prepare and SubTrack modes both belong to the preparing and

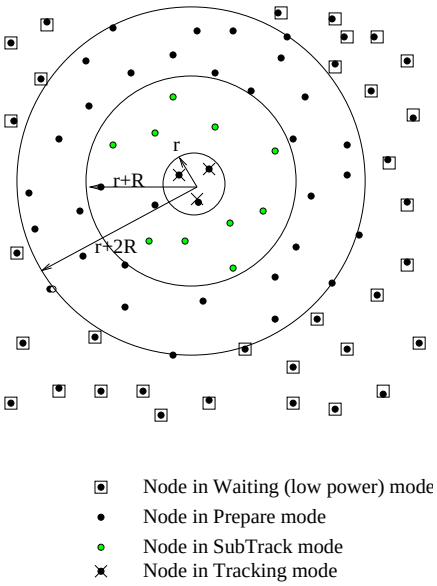

Figure 7: Layered onion-like node state distribution around the target.

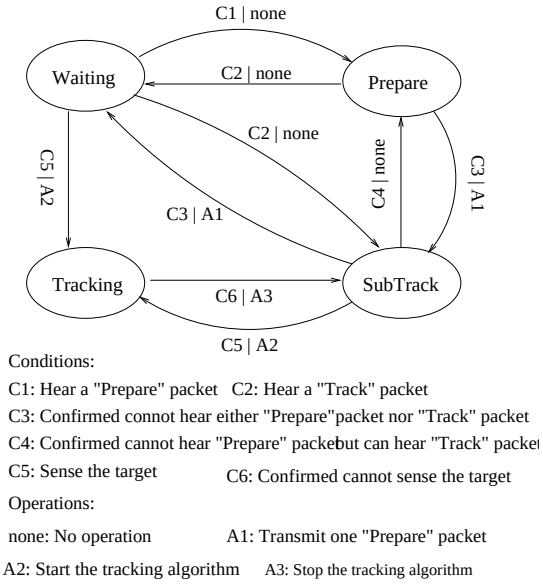

Figure 8: State transition diagram for Tracking Group Management Algorithm.

anticipating mode, and a node should remain active in both modes. Figure 7 shows the layered onion-like node state distribution around the target.

At any given time, if we draw a circle centered at the current location of the target with radius r being the average sensing range, any node that lies within this circle should be in Tracking mode. It actively participates a collaborative tracking operation along with other nodes in the circle. Regardless of the tracking protocol, the tracking nodes form a spatial-temporal local group, and tracking protocol packets are exchanged among the group members. Let us mark these Tracking packets so that any awake node within the transmission range can overhear and identify these packets. Thus, if any node receives Tracking packets but cannot sense any target, it should be aware that a target may be coming in the near future. From the overheard packets, it may also get an estimation of the current location and moving speed vector of the target. The node thus transit into the SubTrack mode from either Waiting mode or Prepare mode. At the boundary, a SubTrack node can be $r + R$ away from the target, where R is the transmission range. To carry the wake-up wave further away, a node should transmit a Prepare packet. Any node that receives a Prepare packet should transit into Prepare mode from Waiting mode. A Prepare node can be as far as $r + 2R$ away from the target.

Figure 8 shows the state transition diagram of the Proactive-Wakeup (PW) algorithm. If a Tracking node confirms that it can no longer sense the target, it transits into the SubTrack mode. Further, if it later confirms that it can no longer receive any Tracking packet, it transits into the Prepare mode. Finally, if it confirms that it can receive neither Tracking nor Prepare packet, it transits back into the Waiting mode. Thus, a tracking node gradually turns back into low power surveillance stage when the target moves further away from it. In essense, the PW algorithm and makes sure that the tracking group is moving along with the target.

6. PERFORMANCE EVALUATION

We use GloMoSim[22] simulator for the performance evaluations. At the physical layer, GloMoSim uses a comprehensive radio model that accounts for noise power, signal propagation and reception. In all the following simulations, the radio propagation model is chosen as the *Two-Ray* pathloss model. To configure the radio interfaces, we setup the following two parameters. The transmitting power is 10 dBm (10 mW). The receiving sensitivity, which is the measure of the lowest signal power that may be reliably received by the receiver, is set as -65 dBm (0.3 μW). With these settings, the typical transmission range in the GloMoSim simulator is 55.9 meters. We set the sensing range of each sensor as 20 meters.

Table 1: Parameters for tuning in sleeping protocols

Protocol	Parameters
RIS	slot time, alertness
PEAS	probe range
PECAS	probe range, WORK_TIME_DUR
GAF	grid size, sleep time, discovery time
MESH	grid size

The sleeping protocols we have implemented are RIS, PECAS, GAF, and MESH. We are not only interested in comparing their relative pro-and-cons, but also explore how to tune the parameters of each protocol. The parameters for tuning are listed in Table 1.

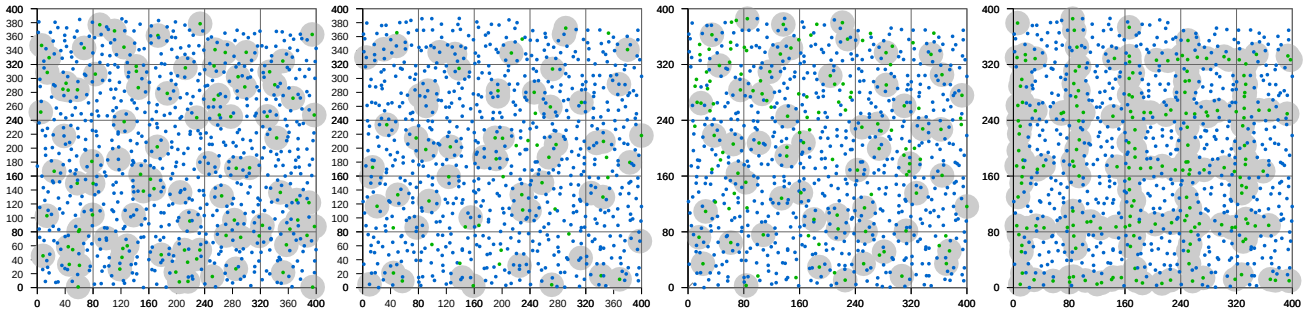

(a) RIS, 98 active nodes. Slot time = 4.0 Second Alertness = 0.125

(b) PECAS, 59 active nodes. Slot time = 10.0 Second Probe range = 50 meter

(c) GAF, 58 active nodes. T_s = 4.0 Second, T_d = 2.0 Second Grid size = 80 meter

(d) MESH, 190 active nodes. Slot time = 4.0 Second Grid size = 80 meter

Figure 9: Spatial distribution of active nodes under all four sleeping protocols.

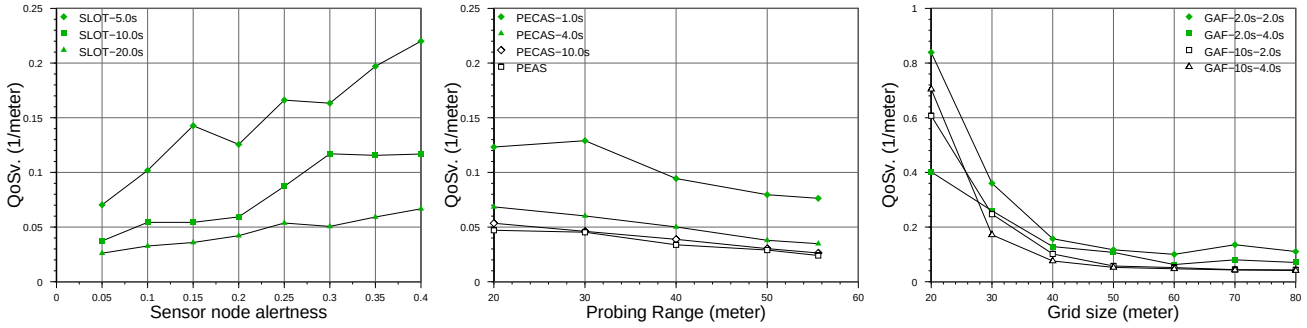

(a) QoSv using RIS.

(b) QoSv using PEAS and PECAS.

(c) QoSv using GAF.

Figure 10: Quality of surveillance under three sleeping protocols (RIS, PECAS, GAF).

6.1 Quality of Surveillance (QoSv)

6.1.1 Simulation Setup

The network field is a free space of size $400m \times 400m$. When tunning parameters within each protocol, we use 800 nodes with uniformly random distribution.

The target appears in the field at a random location. It chooses a random direction and moves in a straight line along the direction, at a speed of 10 m/s. The simulation stops when the target is first detected by a sensor. For each simulation setup, we run 100 times with different random target locations and moving directions, and record the value of undetected moving distance.

6.1.2 Spatial Patterns

A typical scene of spatial distribution of active nodes and the covered area using all four sleeping protocols are shown in Figure 9. Each sensor's covered area is shown as a gray disc. With RIS scheme, since there is no collaboration between neighboring nodes, we can see places where active nodes are densely clustered, as shown in Figure 9(a). This will reduce the QoSv value. For the two neighborhood collaboration methods, GAF and PEAS, the protocols have a scheme to let the active nodes to suppress other nodes in its range to become active. However, from Figures 9(b) and 9(c), we can see they cannot prevent overlap of covered areas. This result is due to the delay of the suppressing process. Figure 9(c) shows that there are multiple active nodes in many grids. This is because the grid size is much greater than the transmission range. In Figure 9(d), a 2-D mesh is roughly formed by the active nodes.

6.1.3 Parameter Tunning in RIS

Figure 10(a) shows the network's QoSv for the RIS protocol. We change the nodal alertness, the percentage of time each node is awake within each time slot, from 0.05 to 0.4. With 800 deployed nodes and alertness higher than 0.4, the active nodes at any time fully cover the field, and the QoSv value is very high. The length of a time slot is set with the following values: 5.0 sec, 10.0 sec and 20.0 sec.

When the nodal alertness starts from 0.05 and increases, the QoSv value increases, because of the shrinking of uncovered areas as the number of active nodes at any given time increases. The QoSv also decreases with the increase of slot time for the same alertness value. With shorter slot time, the work and sleep periods at each node are shorter, the resulting working node set will change more dramatically over time. This more dynamically changing set of working nodes will have higher chance to detect a target. Let us also study the average uncovered distance, namely $\frac{1}{QoSv(X)}$. For shorter slot time, there is little difference of ALUL value

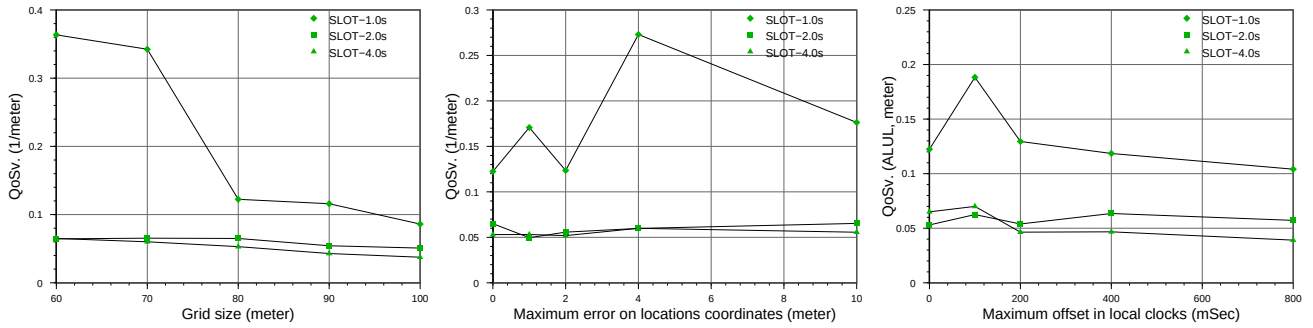

(a) QoSv wrt. mesh grid size. (b) QoSv wrt. localization error. (c) QoSv (ALUL) wrt. time synchronization error.

Figure 11: Quality of surveillance under 2-D mesh planned sleeping protocol.

between low alertness and high alertness, which is also an indication of the effect of constant change of active nodes.

6.1.4 *Parameter Tunning in PEAS/PECAS*

Figure 10(b) shows the network's QoSv using PEAS and PECAS protocols. We change the probe range radius from the sensing range (20 meters) to the transmission range (56 meters). Another tuning parameter is the working time duration of the nodes, which is set as 1.0 sec, 4.0 sec and 10 sec. If we set the parameter to infinity, the PECAS protocol becomes PEAS protocol.

As we increase the probing range, we can observe that the QoSv value decreases. This is the result of decreased number of active nodes in the field at any given time. However, the decrease of QoSv is far slower than the expectation. In theory, the probing area increases as a quadratic function with the probing range, resulting in the rapid decrease in average number of working nodes. However, in the experiments, the number of working nodes does not observe such a rapid decrease. The reason is that the PECAS scheme sometimes fails to prevent all the probing node in a working node's probing range from entering the working mode, which results in multiple working nodes in some probing areas.

The QoSv is lower with longer work period. The reason is similar to the case of RIS scheme with longer slot time. With PEAS, the set of active nodes will not change during the simulation run. However, when we raise the work period to 10 seconds, PECAS performs very close to PEAS protocol. Thus we conclude that for better QoSv, it is advantageous to have shorter work period.

6.1.5 *Parameter Tunning in GAF*

The network's QoSv performance using GAF protocol is shown in Figure 10(c). We change the grid size from 20m to 80m. The GAF protocol has three additional parameters; T_s,T_d and T_a. They are the time a node will stay in Sleep state, Discovery state and Active state, respectively. According to GAF implementation, T_a is decided by the current residual energy. Thus, we can tune the other two parameters, which will affect the distribution of active nodes. In the legend of the figure, "GAF-x-y" means that T_s is x seconds and T_d is y seconds.

As shown in the figure, if we change T_s from 2.0 sec to 10.0 sec, the QoSv value decreases. The reason is that each node will be less frequent to change into Discovery state, which is intended for checking if it should be active and thus becomes a grid head. The distribution of active nodes is less frequent to change during any given time period. On the other hand, if we change T_d from 2.0 sec to 4.0 sec, the QoSv value decreases. The reason is that a node in Discovery state will change to Active state only if it cannot hear from a better grid head candidate for T_d sec. With longer T_d, a node will be less probable of becoming active.

A notable observation is that the QoSv value no longer decreases with the increase of grid size, when the grid size is greater than the transmission range (55.9 m). In large grids, multiple active nodes will appear in one grid. Thus, at this point, the density of active nodes cannot be controlled by grid size. However, T_s and T_d parameters still affects QoSv significantly.

6.1.6 *QoSv and Parameter Tunning in MESH*

The performance results for 2-D MESH sleeping protocol are shown in Figure 11. With this protocol, we not only study the QoSv performance with regard to grid size, but also study how the errors in localization and time synchronization will affect the network's QoSv performance. The vertical and horizontal virtual lines in the field are 10 meters width. Only nodes that are located on the lines will be active. At the beginning of each time slot, a new set of virtual lines will replace the old ones so that the nodes can switch roles of being active. The length of time slots are set as the following values: 1.0 sec, 2.0 sec and 4.0 sec.

Figure 11(a) shows that QoSv value decreases with the increase of grid size. Each grid contains just one uncovered region. With larger grid size, the number of uncovered region reduces, but the size of each region increases. This is less advantageous in detection when there are more but smaller uncovered regions, which happens when the grid size is smaller. The impact of slot time, which affects the QoSv performance in the same manner as it does in other three sleeping protocols, is also shown in this figure.

We introduce localization errors, and study if the sleeping protocol is susceptible to it. The coordinate values known

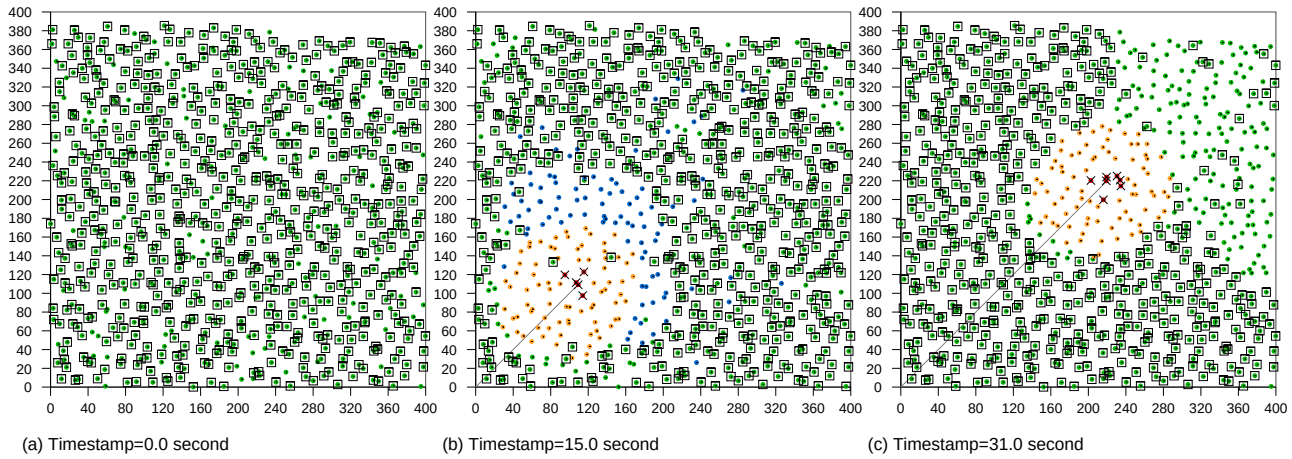

Figure 12: Snap-shots in the simulation run.

to each sensor is a result of applying an offset to the actual values. The offset is an uniform random value between zero and a maximum. In Figure 11(b), we change the maximum error value from 0 to 10m. At 2.0 sec and 4.0 sec slot times, the plots in the figure indicates that localization error has a small impact on QoSv. Thus, we conclude that, with longer slot times, the MESH sleeping protocol is robust against localization errors, even though the protocol needs location information for sleep decision.

The impact of time synchronization errors are shown in Figure 11(c). The clock value known to each sensor is a result of applying an offset to the actual simulation clock. The offset at each sensor is an uniform random value between zero and a maximum. We change the maximum offset from 0 to 800 mSec. From the figure, we also observe a very small impact of synchronization errors. The QoSv is even better at certain offset values. This phenomenon occurs at all three slot time values. The synchronization errors hurts the formation of virtual lines for the distribution of active nodes, and the uncovered regions becomes more irregular. However, simulation study shows that the randomness introduced may help in target detection. Thus, we conclude that only a light-weight time synchronization is enough for the MESH sleeping protocol.

6.2 Integration of Sleep and Wakeup Protocols

We have considered a network field is of size $420m \times 420m$, with 878 sensor nodes uniformly distributed. In the Cartesian space, the coordinate of bottom-left corner and the top-right corner of the field is (-20,-20) and (400,400), respectively. Figure 12 show three scenes of target path and distribution of nodes states within the smaller square area from origin to (400,400). We force the number of sensors in the smaller area to be 800. The target enters the field from the origin point, and moves along the diagonal line towards (400,400) with a constant speed of 10 m/s. In this example, the network is using RIS sleep protocol and proactive wakeup protocol. The nodal alertness is 0.1.

The following metrics are used for considering the protocol performance.

1. Energy savings: The total consumed energy for all nodes during a simulation run in the non-sleeping case minus the total consumed energy with sleeping is the amount of energy savings. The value divided by the total consumed energy in non-sleeping case is relative energy saving.

2. Target path exposure: This follows the *Path Exposure* definition in [14], which is the integral of the network's sensing intensity function at each point along the path. In this experiment, the sensing intensity of a sensor x at point p is defined as $s(x,p) = \frac{1}{|x,p|^4}$. And the network's sensing intensity at point p is the sensing intensity measure from the closest working sensor in the field to point p. One addition to the definition is that a sleeping node will have zero sensing intensity over any point.

We implemented both random independent sleeping (RIS) and PECAS scheme for neighborhood collaborative sleeping. Each sleeping scheme is combined with the proactive wakeup(PW) scheme. This makes two sleep-wakeup scheme combinations, and they are named RIS-PW and PECAS-PW, respectively.

6.2.1 *Energy Savings*

In this section, we study the percentage of energy savings by applying sleep planing schemes. The results of applying RIS-PW and PECAS-PW schemes are shown in Figures 13(a) and 13(b), respectively.

When applying the RIS scheme, we control the average number of working sensors by changing the sensor node alertness, which is defined as the percentage of working period within each time slot. Figure 13(a) shows the relative energy saving as a function of node alertness under different length of slot time. The results show that the energy saving is briefly

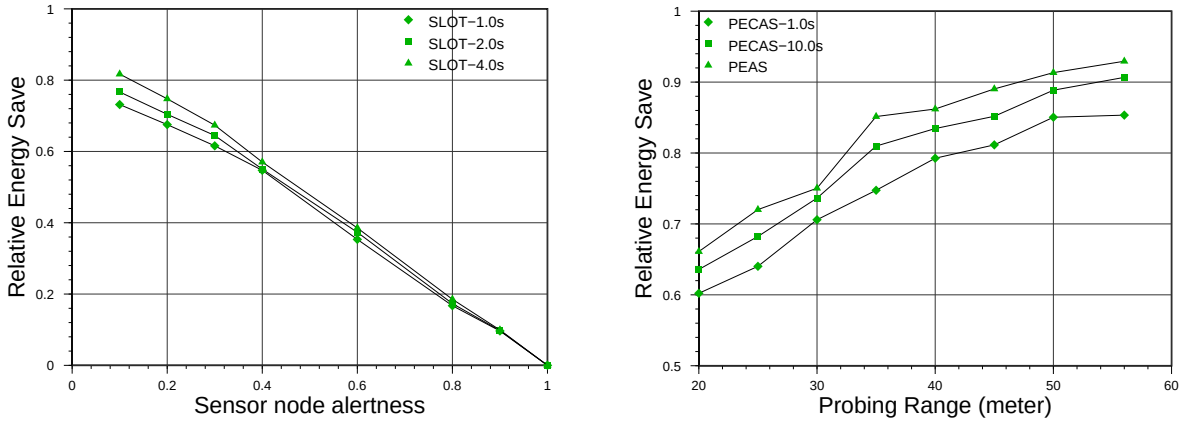

(a) Random independent sleeping.

(b) Neighborhood collaborative sleeping.

Figure 13: Relative energy saving.

in linear relation with the node alertness index. The total energy consumption is composed of the energy used for sensing and listening to the radio channel, and that used for control traffic incurred by the Proactive Wakeup (PW) protocol and tracking protocol. Since the later part is spatially and temporally constrained to a small fraction of sensors, it only constitutes a small fraction of total energy consumption. Altering slot time does not make much difference in energy saving. We are more interested in the cases of smaller alertness values, which translates to more sleeping. Longer slot time yields deeper energy savings. However, as shown in other simulation results, the QoSv and path exposure are both low in this case.

Figure 13(b) shows the energy savings by applying PECAS scheme. The number of working nodes is controlled by the probing range. Parameter *Work_Time_Dur* is the length of each working period. Results with 1.0 second, 10.0 second and infinity(PEAS) work periods are shown in the figure. We vary the probing range from the sensing range to the packet transmission range, which are 20m and 55.9m, respectively. The figure shows significant energy savings. For example, with probing range twice the sensing range (at 40m), the energy savings are 79.2% , 83.4% and 86.2% for 1.0 second, 10.0 second and infinity(PEAS) work periods, respectively. The energy saving is greater with longer work period. This is because with longer work period, Collaborated Adaptive Sleeping (CAS) scheme will prolong the sleeping periods as well. This will result in significantly less Probing/Reply dialogs. However, the difference is not as significant, which indicates the energy for control traffic is relatively minor compared the energy for sensing and listening.

6.2.2 *Target Path Exposure*

From the definition, one can see that target path exposure is the amount of sensing intensity the target cumulatively receives while traversing the path in the network field. Higher value of exposure will indicate better quality of tracking of the network along the path. If the sensors are sleeping while a target passes by, it does not contribute to the sensing intensity value. The proactive wakeup scheme alerts the sensors to be prepared for an approaching target. Ideally, the exposure of the path in a field with either RIS-PW or PECAS-PW schemes will be the same as the exposure in a non-sleeping field.

Figure 14(a) shows the results for applying RIS-PW scheme. When the alertness value equals 1, which means in the non-sleeping case, the exposure is at highest value 4.835. As the alertness value decreases to 0.1, the exposure value decreases as well. The reason for this behavior is that it is harder to proactively wakeup all sensor nodes in a given region when each sensor spends more fraction of time in sleeping, which is indicated by lower alertness values. We can also observe that shorter slot time will alleviate the situation. As each sensor wakes up more frequently under shorter slot time, there is more chances for a sensor to be alerted by the proactive wakeup scheme.

The results for applying PECAS-PW scheme under different work period lengths are shown in Figure 14(b). The case with infinity work period is equivalent to the PEAS protocol. It can be observed that the exposure value increases with shorter probing range or with shorter work period length. The reason for this is similar to the case of RIS-PW schemes. The path exposure value for PEAS is much lower than PECAS schemes. The reason is that as work period get longer, the inactive nodes will sleep longer between wake-ups, which makes it more difficult for the proactive wakeup scheme to take effect.

7. CONCLUSIONS

A detailed study of the trade-off analysis between power consumption and quality of surveillance is presented in this paper. We have formalized the quality of surveillance issues

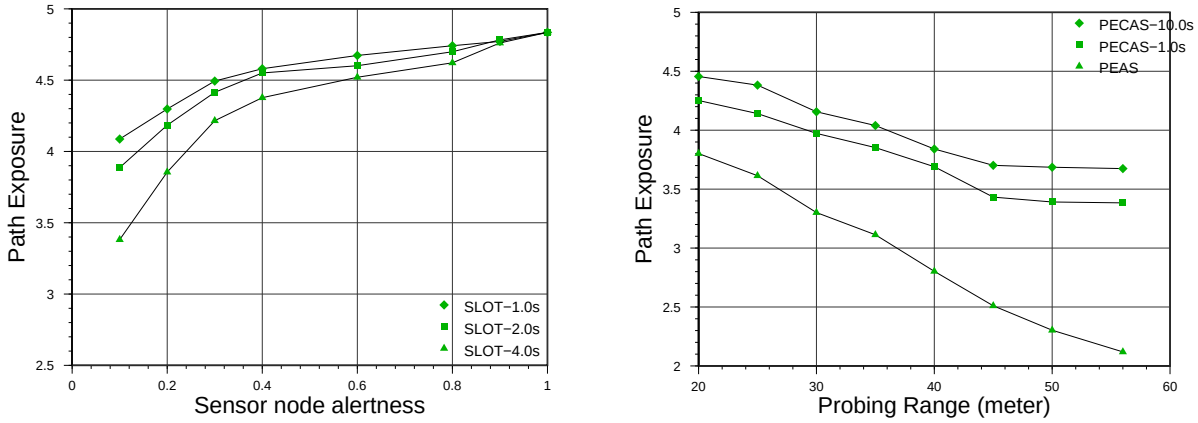

(a) Random independent sleeping.

(b) Neighborhood collaborative sleeping.

Figure 14: Comparing the path exposure.

in the target tracking sensor networks and have develop a model for quantifying meaningful metrics for the quality of surveillance. In addition, we have develop efficient sleep-awake protocols, called PECAS and MESH, that provide high quality of surveillance while minimizing the power consumption. Using the model for quality of surveillance and the sleep-awake protocol, we propose efficient deployment guidelines for sensor node in target tracking applications. The quality of surveillance metric for the deployment techniques are derived analytically. Our proposed approaches and models are motivated and evaluated through detailed simulations. The results demonstrate the trade-off analysis and quantifies the benefit through comparisson with other techniques. Our future efforts will be on the issues involved in tracking multiple targets.

8. REFERENCES

[1] J. Aslam, Z. Butler, V. Crespi, G. Cybenko, and D. Rus. Tracking a moving object with a binary sensor network. In *ACM International Conference on Embedded Networked Sensor Systems(SenSys)*, 2003.

[2] M. Cardei, D. MacCallum, X. Cheng, M Min, X. Jia, D. Li, and D.-Z. Du. Wireless sensor networks with energy efficient organization. *Journal of Interconnection Networks*, 3(3-4), 2002.

[3] M. Cardei and J. Wu. *Handbook of Sensor Networks*, chapter Coverage in Wireless Sensor Networks. CRC Press, 2004.

[4] A. Cerpa and D. Estrin. Ascent: Adaptive self-configuring sensor networks topologies. In *IEEE Infocom*, 2002.

[5] K. Chakrabarty, S.S. Iyengar, H. Qi, and E. Cho. Grid coverage for surveillance and target location in distributed sensor networks. *IEEE Transaction on Computers*, 51(12), 2002.

[6] B. Chen, K. Jamieson, and H. Balakrishnan. Span: An energy efficient coordination algorithm for topology maintenance in ad hoc wireless network. In *ACM Mobicom*, 2001.

[7] M. Chu, H. Haussecker, and F. Zhao. Scalable information-driven sensor querying and routing for ad hoc heterogeneous sensor netoworks. *International Journal on High Performance Conputing Applications*, 16(3), 2002.

[8] Saurabh Ganeriwal, Ram Kumar, Sachin Adlakha, and Mani Srivastava. Network-wide time synchronization in sensor networks. Technical report, UCLA, April 2002.

[9] E.N. Gilbert. Random plane networks. *Journal of Social and Industrial Applied Math.*, 9, 1961.

[10] Peter Hall. On continuum percolation. *The Annals of Probability*, 13(4), 1985.

[11] Peter Hall. *Introduction to the Theory of Coverage Processs*. John Wiley and Sons, Inc., 1988.

[12] C.F. Huang and Y.C. Tseng. The coverage problem in a wireless sensor network. In *ACM Workshop on Wireless Sensor Networks and Applications (WSNA)*, 2003.

[13] K. Mechitov, S. Sundresh, Y. Kwon, and G. Agha. Cooperative tracking with binary-detection sensor networks. Technical Report UIUCDCS-R-2003-2379, Computer Science Dept., University of Illinois at Urbana-Champaign, 2003.

[14] S. Megerian, F. Koushanfar, G. Qu, and M. Potkonjak. Exposure in wireless sensor networks. In *ACM International Conference on Mobile Computing and Networking (Mobicom)*, 2001.

[15] S. Meguerdichian, F. Koushanfar, M. Potkonjak, and M. B. Srivastava. Coverage problems in wireless ad-hoc sensor networks. In *IEEE Infocom*, 2001.

[16] J. Pan, Y. T. Hou, L. Cai, Y. Shi, and S. X. Shen. Topology control for wireless sensor networks. In *ACM Mobicom*, 2003.

[17] S. Pattem, S. Poduri, and B. Krishnamachari. Energy-quality tradeoffs for target tracking in wireless sensor networks. In *International Workshop on Information Processing in Sensor Networks (IPSN)*, 2003.

[18] C. Schurgers, V. Tsiatsis, S. Ganeriwal, and M. Srivastava. Optimizing sensor networks in the energy-latency-density design space. *IEEE Trans. Mobile Computing*, 1(1), 2002.

[19] R. W. Sittler. An optimal data association problem in surrveillance theory. *IEEE Trans. on Military Electronics*, april 1964.

[20] S. Slijepcevic and M. Potkonjak. Power efficient organization of wireless sensor networks. In *IEEE International Conference on Communication*, 2001.

[21] S. Tilak, N. Abu-Ghazaleh, and W. Heinzelman. A taxonomy of wireless micro-sensor network models. *Mobile Computing and Communications Review (MC2R)*, 6(2), 2002.

[22] UCLA. Glomosim. http://pcl.cs.ucla.edu/projects/glomosim.

[23] Jana van Greunen and Jan Rabaey. Lightweight time synchronization for sensor networks. In *ACM International Workshop on Wireless Sensor Network and Applications*, 2003.

[24] G. Veltri, Q. Huang, G. Qu, and M. Potkonjak. Minimal and maximal exposure path algorithms for wireless embedded sensor networks. In *ACM International Conference on Embedded Networked Sensor Systems(SenSys)*, 2003.

[25] Q.X. Wang, W.P. Chen, R. Zheng, K. Lee, and L. Sha. Acoustic target tracking using tiny wireless sensor devices. In *International Workshop on Information Processing in Sensor Networks (IPSN)*, 2003.

[26] X. Wang, G. Xing, Y. Zhang, C. Lu, R. Pless, and C. Gill. Integrated coverage and connectivity configuration in wireless sensor networks. In *ACM International Conference on Embedded Networked Sensor Systems(SenSys)*, 2003.

[27] Y. Xu, J. Heidemann, and D. Estrin. Geography informed energy conservation for ad hoc routing. In *ACM Mobicom*, 2001.

[28] T. Yan, T. He, and J.A. Stankovic. Differentiated surveillance of sensor networks. In *ACM International Conference on Embedded Networked Sensor Systems(SenSys)*, 2003.

[29] H. Yang and B. Sikdar. A protocol for tracking mobile targets using sensor networks. In *IEEE International Workshop on Sensor Networks Protocols and Applications*, 2003.

[30] F. Ye, G. Zhong, J. Cheng, S.W. Lu, and L.X. Zhang. Peas:a robust energy conserving protocol for long-lived sensor networks. In *IEEE International Conference on Distributed Computing Systems(ICDCS)*, 2003.

[31] W. Zhang and G. Cao. Dctc: Dynamic convoy tree-based collaboration for target tracking in sensor networks. *IEEE Trans. on Wireless Communications*, 2004.

[32] W. Zhang and G. Cao. Optimizing tree reconfiguration for mobile target tracking in sensor networks. In *IEEE Infocom*, 2004.

[33] F. Zhao, J. Shin, and J. Reich. Information-driven dynamic sensor collaboration for tracking applications. *IEEE Signal Processing Magazine*, March 2002.